

**MOLECULAR DYNAMICS SIMULATION OF  
PDMS NANOSTRUCTURE DISTORTION IN SOFT  
LITHOGRAPHY DEMOLDING PROCESS**

**ABDUL HAADI BIN ABDUL MANAP**

**UNIVERSITI SAINS MALAYSIA**

**2021**

**MOLECULAR DYNAMICS SIMULATION OF  
PDMS NANOSTRUCTURE DISTORTION IN SOFT  
LITHOGRAPHY DEMOLDING PROCESS**

by

**ABDUL HAADI BIN ABDUL MANAP**

**Thesis submitted in fulfilment of the requirements  
for the degree of  
Doctor of Philosophy**

**AUGUST 2021**

## ACKNOWLEDGEMENT

I want to express my deepest gratitude to Associate Professor Dr Khairudin Mohamed, my supervisor, for his guidance, encouragement, patient and assistance. He not only guides me throughout this project but also inspired continuously and motivated me to continue this research. This thesis would be not possible to complete without his assistance. I also want to thanks my parent Abdul Manap Bin Abdul Ghani and Sarifah Radziah Binti Ali and all my friends for their support and encouragement. I would also like to extend my gratitude to all the lecturers and administrative staff in the School of Mechanical Engineering (Pusat Pengajian Kejuruteraan Mekanik), Universiti Sains Malaysia help and guidance throughout my study here. This project would not be possible if not for the financial funding from Rancangan Latihan Akademi (RLKA ) programme supported by Universiti Sains Malaysia. This thesis is not possible if not for the open-source community that help provide software and tools for this research. I would like to say thank you for all the developers and coders for Large-scale Atomic/Molecular Massively Parallel Simulator (LAMMPS), open-source Java viewer for 3d chemical structures (JMOL), Molecular Dynamics Packing Optimization Software (Packmol) and all contributors in Python Library. Finally, I would like to give special remarks to my wife, Nurhayati Binti Eszer because of all of her sacrifice and never-ending support and encouragement. For my son Abdul Kareem bin Abdul Haadi and my daughter Nur Raudahtul Jannah Binti Abdul Haadi, thanks for the sanity pill you give when your father lost his way. Alhamdulillah.

## TABLE OF CONTENTS

<b>ACKNOWLEDGEMENT.....</b>	<b>ii</b>
<b>TABLE OF CONTENTS.....</b>	<b>iii</b>
<b>LIST OF TABLES.....</b>	<b>vi</b>
<b>LIST OF FIGURES.....</b>	<b>vii</b>
<b>LIST OF SYMBOLS.....</b>	<b>x</b>
<b>LIST OF ABBREVIATIONS.....</b>	<b>xi</b>
<b>LIST OF APPENDICES.....</b>	<b>xiv</b>
<b>ABSTRAK.....</b>	<b>xv</b>
<b>ABSTRACT.....</b>	<b>xvii</b>
<b>CHAPTER 1 INTRODUCTION.....</b>	<b>1</b>
1.1 Introduction.....	1
1.2 Research background.....	2
1.3 Problem statement .....	4
1.4 Research objective .....	5
1.5 Scope of research .....	5
1.6 Thesis outline .....	6
<b>CHAPTER 2 LITERATURE REVIEW.....</b>	<b>8</b>
2.1 Introduction.....	8
2.2 Soft lithography and its applications .....	8
2.2.1 Development in cell-nanotopography interaction and its application .....	15
2.2.2 Polydimethylsiloxane in Soft Lithography.....	24
2.3 Nanostructure distortion in the demolding process .....	25
2.4 Molecular dynamics simulation in soft lithography .....	28
2.5 Force field in molecular dynamics simulation .....	28

2.5.1	Polymer consistent force field (PCFF).....	29
2.5.2	Condensed-phase optimized molecular potential for atomistic simulation studies force field (COMPASS) .....	30
2.6	Summary.....	30
<b>CHAPTER 3 METHODOLOGY.....</b>		<b>32</b>
3.1	Introduction.....	32
3.2	Experimental method.....	32
3.2.1	Sample Preparation .....	32
3.2.1(a)	Photoresist Preparation .....	34
3.2.1(b)	Photoresist Coating.....	34
3.2.2	EBL Setup .....	35
3.2.2(a)	Pattern Design .....	35
3.2.2(b)	Position Alignment .....	36
3.2.2(c)	Beam Focusing or Turning.....	38
3.2.2(d)	Pattern Exposure Condition.....	38
3.2.3	Pattern Development process.....	39
3.2.4	PDMS replication.....	40
3.3	Simulation Method .....	40
3.3.1	Building block for substrate .....	41
3.3.1(a)	Building block for PDMS nanopillar and nanocones 42	
3.3.2	Simulation modelling .....	44
3.3.2(a)	Governing equation and calculation method.....	45
3.3.3	Initial condition.....	51
3.3.4	Boundary Condition .....	52
3.3.5	Energy minimization .....	54
3.3.6	Equilibrium.....	56
3.4	Summary.....	57

<b>CHAPTER 4</b>	<b>RESULTS AND DISCUSSIONS.....</b>	<b>59</b>
4.1	Introduction.....	59
4.2	Experimental Results .....	60
4.3	Molecular dynamics results .....	66
4.3.1	Energy Minimization.....	66
4.3.2	Substrate equilibrium .....	69
4.3.2(a)	Temperature equilibrium.....	69
4.3.2(b)	Pressure equilibrium .....	71
4.3.3	Nanostructure under tension .....	73
4.3.3(a)	Visual observation of nanostructure deformation .....	74
4.3.4	The effect of chain length on the stress and strain relationship .....	76
4.3.5	The effect of temperature on stress and strain relationship .....	83
4.4	Summary .....	87
<b>CHAPTER 5.....</b>	<b>.....</b>	<b>90</b>
<b>CONCLUSION AND RECOMMENDATIONS .....</b>	<b>.....</b>	<b>90</b>
5.1	Conclusion .....	90
5.2	Recommendation.....	93
<b>REFERENCES.....</b>	<b>.....</b>	<b>94</b>
APPENDICES		
LIST OF PUBLICATIONS		
LIST OF CONFERENCES		

## LIST OF TABLES

	<b>Page</b>
Table 2-1	Summary of various studies that using different technique of nanoimprint lithography .....14
Table 2-2	Summary of cell response to precise,highly symmetric nanostructures.....19
Table 2-3	Summary of cell response to randomize nanostructures .....20
Table 2-4	Summary of cell response to disorder/irregular nanostructure .....22
Table 2-3	Type of deformation in the demolding process .....26
Table 4-1	Mechanical properties of PDMS substrate under tension .....81
Table 4-2	Mechanical properties of PDMS substrate under tension at difference temperature.....84

## LIST OF FIGURES

		<b>Page</b>
Figure 2.1	Soft lithography uses in NIL a) Imprint process and b) Demolding process .....	9
Figure 2.2	Comparison of Thermal Nanoimprint Lithography (Thermal NIL) and Ultra-Violet Nanoimprint Lithography (UV NIL) .....	11
Figure 2.3	Nanoimprint variation based on imprint techniques .....	13
Figure 2.4	Factors that cause dimensional instability and its effect .....	27
Figure 3.1	Workflow of nanofabrication process .....	33
Figure 3.2	(A) PDMS Chemical Structure and (B) illustration of PDMS monomer .....	42
Figure 3.3	(A) PDMS monomer (B) PDMS substrate with dimension is 1000Å, 1000Å, 1000Å in x,y and z direction.....	43
Figure 3.4	PDMS nanocones model with dimension -2.565Å, -127.263Å, -53.273Å to 253.16Å, 127.373Å, 53.273Å in x, y, z directions .....	43
Figure 3.5	Computational, Time/Length Scale and Applications .....	44
Figure 3.6	The process flow of the calculation in typical molecular dynamic simulation.....	45
Figure 3.7	Process summary for step 1 and 2 .....	46
Figure 3.8	An atoms with it neighbouring radius .....	49
Figure 3.9	Periodic boundary conditions in 2 dimensions. The cell in the center is the main simulation box.....	53
Figure 3.10	Cell (bin) where primary cell at center of the simulation box .....	53
Figure 3.11	Generic pattern on energy minimization chart .....	56
Figure 4.1	(A) PDMS replica with base dimension 140nm, height 40nm and pitch 850nm and (B) PMMA mold with base dimension 157nm, depth 90nm and pitch 785nm.....	61



Figure 4.2	Height and width profile of PDMS replica and PMMA mold in Figure 4.1 .....	62
Figure 4.3	(A) Fabricate mold with base dimension 118nm, depth 30nm and pitch 235nm and (B) PDMS replica with base dimension 176nm, height 40nm and pitch 157nm.....	63
Figure 4.4	Height and width profile of PDMS replica and PMMA mold in Figure 4.4 .....	64
Figure 4.5	(A) PDMS replica with base dimension 280nm, height 150nm and pitch 800nm and (B)PMMA mold with base dimension 235nm, depth 80nm and pitch 850nm.....	65
Figure 4.6	Height and width profile of PDMS replica and PMMA mold in Figure 4.5 .....	66
Figure 4.7	Energy Minimization graph using the COMPASS force field .....	68
Figure 4.8	Energy Minimization graph using the PCFF force field .....	68
Figure 4.9	Temperature equilibrium using COMPASS forcefield .....	70
Figure 4.10	Temperature equilibrium using PCFF forcefield .....	70
Figure 4.11	Pressure equilibrium using COMPASS forcefield .....	71
Figure 4.12	Pressure equilibrium using COMPASS forcefield close-up.....	72
Figure 4.13	Pressure equilibrium using PCFF forcefield .....	72
Figure 4.14	Pressure equilibrium using PCFF forcefield close-up.....	73
Figure 4.15	PDMS nanopillar stretch at strain A) 0.0, B) 0.1, C) 0.4 .....	75
Figure 4.16	PDMS nanocones stretch at uniaxial strain (A) 0.0 (B) 0.1 (C) 0.4 ...	76
Figure 4.17	Stress-strain curve of PDMS with 8 and 12 chain monomer using COMPASS .....	79
Figure 4.18	Stress-strain curve of PDMS with 8 and 12 chain monomer using PCFF forcefield .....	80
Figure 4.19	Stress-strain curve of PDMS with 8 and 12 chain monomer using PCFF forcefield .....	82

Figure 4.20	Stress-strain curve of PDMS nanocones using PCFF and COMPASS force field at T=300K .....	84
Figure 4.21	Stress-strain curve of PDMS nanocones using PCFF and COMPASS force field at T=310K .....	85
Figure 4.22	Stress-strain curve of PDMS nanocones using PCFF and COMPASS force field at T=320K .....	85
Figure 4.23	Stress-strain curve for PDMS nanocones using (A) PCFF forcefield (B) .....	87

## LIST OF SYMBOLS

$T_s$	Substrate Temperature	K
$T_g$	Glass transition temperature	K
$E_{\text{non-bonded}}$	Non-Bonded Energy	$\text{kgm}^2\text{s}^{-2}$
$E_{\text{valence}}$	Valence Energy	$\text{kgm}^2\text{s}^{-2}$
$\Delta t$	Timestep	s
$p$	Momentum	$\text{kgms}^{-1}$
$F_i$	Interaction Force	$\text{kgms}^{-2}$
$U_b$	Sublimation energy	$\text{kgm}^2\text{s}^{-2}$
$O(\delta t^4)$	Truncation error	-
$v(t)$	Velocity	$\text{ms}^{-1}$
$a(t)$	Acceleration	$\text{ms}^{-2}$
$A(\Gamma(t))$	Function of phase time	-
$2r_0$	Initial distance between two atoms.	m
$x(t)$	Position	m
$E_p$	Potential Energy	$\text{kgm}^2\text{s}^{-2}$

### *Greek Symbol*

$\alpha$	Alpha	
$\varepsilon$	Reduced energy	
$\alpha^*$	Function of mass ratio	
$\tau$	coupling constant of $\frac{M_2}{M_1}$	
$d_f$	Fiber diameter	
$A_{\text{ellipse}}$	Ellipse-shaped aspect ration	

## LIST OF ABBREVIATIONS

ASL	Anti-sticking layer
BD	Brownian Dynamics
C	Carbon
CA	Cellulose Acetate
CFD	Computational Fluid Dynamics
COMPASS	Condensed-phase Optimized Molecular Potentials for Atomistic Simulation Studies
CSK	Intracellular actin cytoskeleton
DBSA	Dodecylbenzenesulphonic Acid
DEX	Dexamethosane
DFT	Density Functional Theory
DPD	Dissipative Particle Dynamics
DSQ20	Disordered square array with dots displaced randomly by up to 20nm on both axes from their position in a true square
DSQ50	Disordered square array with dots displaced randomly by up to 50nm on both axes from their position in a true square
ETFE	Ethylene Tetrafluoroethylene
FEA	Finite Elements Analysis
FEV	Finite Volume Analysis
FNC	Mixture Of Fibronectin And Collagen
GDC	Gadolinium-doped ceria
GNMS	Hexaganol graphene nanomesh
H	Hydrogen
HCECs	Human Corneal Endothelial Cells
HEX	Hexagonal array
hFOB	Human fetal osteoblast

HSQ	Hydrogensilsesquioxane
hMSCs	Human Mesenchymal Cells
HUVECS	Human Umbilical Endothelial Cells
LAMMPS	Large-scale Atomic/Molecular Massively Parallel Simulator
LC	Mixture Of Laminin (Gibco) And Chondroitin Sulfate (Sigma)
MC	Monte Carlo
MC3T3-E1	Mouse osteoblastic cell line
MD	Molecular Dynamics
MEMs	Microelectromechanical Systems
MG-63	Osteoblast-like-cell
MSCs	Mesenchymal Cells
NC	Nerve cells
NEMs	Nanoelectromechanical Systems
NI	Nickel
NIH/3T3	Mouse embryonic fibroblast cells
NIL	Nanoimprint Lithography
NPT	mol,pressure and temperature
NVE	mol,volume and energy
O	Oxygen
P2P	Plate-to-plate
PANI	Polyaniline
PBC	Periodic boundaries conditions
PCFF	Polymer Consistent Forcefield
PDMS	Poly(dimethylsiloxane)
PET	Polyethylene terephthalate
PLLA	Poly(L-lactic acid)
PLGA	Poly(lactic-co-glycolic acid)

PMMA	Poly(methyl methacrylate)
PUA	Polyurethane acrylate
QM	Quantum Mechanics
R2P	Roll-to-plate
RAND	Pits placed randomly over a 150 $\mu\text{m}$ by 150 $\mu\text{m}$ field, repeated to fill a 1 $\text{cm}^2$ area
Si	Silicon
SiO <sub>2</sub>	Silicon Oxide
SQ	Square Array
TCPS	Tissue Cultured Polystyrene
Ti	Titanium
SPH	Smooth Particle Hydrodynamics
UV	Ultraviolet
UV-NIL	Ultraviolet Nanoimprint Lithography
vSMCs	Vascular smooth muscle cells
YSZ(110)	(110) oriented yttria-stabilized zirconia single crystal

## LIST OF APPENDICES

- Appendix A LAMMPS Programming
- Appendix B Datasheet for Polymer Consistent Forcefield (PCFF)
- Appendix C Datasheet for Condensed-phase Optimized Molecular Potentials  
for Atomistic Simulation Studies (COMPASS)

**SIMULASI HEROTAN STRUKTUR PDMS BERSKALA NANO  
DALAM PENCORAKAN LEMBUT DENGAN MENGGUNAKAN KAEDAH  
MOLEKULAR DINAMIK**

**ABSTRAK**

Thesis ini membentangkan hasil kajian tentang herotan struktur berskala nano bahan PDMS yang berlaku semasa proses penyahacuan di dalam teknik pencorakan lembut dengan menggunakan kaedah pengkomputeran. Teknik cetakan nano menggunakan konsep penyesaran bahan dengan menggunakan sentuhan secara mekanikal. Walaupun teknik penyesaran bahan merupakan teknik yang biasa digunakan dalam fabrikasi, namun begitu pada skala kecil terdapat banyak faktor yang boleh menyebabkan berlakunya herotan kepada struktur seperti suhu, tekanan, nilai nisbah aspek, teknik menyalat dan sebagainya. Apabila mengambil kira kesemua faktor yang boleh menyebabkan herotan kepada struktur, ia amat penting untuk memahami hubungan antara penyesaran dan tekanan pada proses penyahacuan. Walaupun terdapat banyak kajian dilakukan untuk mengoptimumkan teknik fabrikasi, namun begitu kebanyakan kajian adalah berbentuk eksperimen yang hanya fokus kepada mengoptimumkan parameter tetapi tidak kajian fundamental. Dalam thesis ini, hasil kajian daripada kaedah pengkomputeran mekanik molekul memberi sudut pandang secara fundamental dan menerangkan proses penyahacuan lembut secara teori. Dua jenis Potensi-Antara-Atom yang digunakan untuk model komputer herotan struktur nano selepas proses penyah-acuan. Potensi Antara Atom tersebut adalah Potensi COMPASS (*Condensed-phase Optimized Molecular Potentials for Atomistic Simulation Studies*) dan Potensi PCFF (*Polymer Consistent Forcefield*). Data daripada kedua-dua potensi antara atom ini akan digunakan untuk mencari hubungan antara



penyesaran dan tekanan pada struktur nano apabila daya dikenakan padanya. Thesis ini membuat kajian terhadap dua jenis nanostruktur iaitu kon berskala nano (nanokon) dan tiang berskala nano (nanotiang). Analisis melalui perbandingan akan dibuat antara hasil kajian daripada teknik pengkomputeran dan eksperimen. Objektif utama thesis ini adalah untuk mencari hubungan antara penyesaran dan tekanan terhadap struktur berskala nano. Ujian eksperimen menunjukkan panjang nanotiang dari material PDMS meningkat sebanyak 10-60% daripada panjang acuan apabila daya regangan dikenakan padanya. Panjang nanokon dari bahan PDMS pula meningkat sebanyak 150-160% daripada panjang acuan asalnya. Pemerhatian daripada hasil eksperimen inilah memberi arah dan asas kepada teknik penkomputeran. Hasil kajian daripada simulasi komputer menunjukkan nanokon pada suhu 300 K, 310 K dan 320 K mempunyai karakteristik seperti plastik fleksibel dan berlaku pemanjangan yang jelas. Tekanan Tertinggi untuk PDMS nanokon pula antara 4.335 MPa - 6.478 MPa. Hasil kajian daripada simulasi komputer juga menunjukkan nanotiang yang menggunakan monomer bersiri 8 dan 12 mempunyai karakteristik seperti plastik fleksibel. PDMS nanotiang mempunyai nilai Young Modulus lebih rendah iaitu 67–71 % daripada nilai daripada PDMS pukal, Tekanan tertinggi juga lebih rendah iaitu 46.3 % lebih rendah daripada PDMS pukal manakala Nisbah Poisson juga lebih rendah iaitu 46.0 % daripada nilai pukal.

# **MOLECULAR DYNAMICS SIMULATION OF PDMS NANOSTRUCTURE DISTORTION IN SOFT LITHOGRAPHY DEMOLDING PROCESS**

## **ABSTRACT**

In this thesis, the distortion of PDMS nanostructures in the demolding process of the soft lithography process was studied and investigated using the computational method. Nanoimprint lithography uses the simple concept of material displacement by mechanical contact. While the idea is simple, many factors may distort the replications, such as temperature, pressure, aspect ratio and peeling-off technique. Thus, when all distortion factors are accumulated, it is crucial in the manufacturing process to understand the stress and strain relationship of materials in the demolding process. Although there are extensive studies and research conducted to optimize the fabrication process, most of them are experimental focusing on the process outcome and parameter optimization rather than the fundamental study of the process. In this thesis, the molecular dynamics simulation method was utilized to fill the gap to breach the fundamental analysis and the process outcome. Two force fields have been used to study the distortions of nanostructures in the demolding process. The force fields are Condensed-phase Optimized Molecular Potentials for Atomistic Simulation Studies (COMPASS) and Polymer Consistent Forcefield (PCFF). The results from these force fields will be utilized to find the nanostructures' stress-strain relationship when forces were applied. This thesis will investigate two types of nanostructures which are nanocones and nanopillar. The results from the simulation will be analyzed and compared with experimental results. This thesis's main interest is to find the stress and strain relationship of the nanostructure and relate it to molecular mechanics.

The experimental results show clear signs of elongation during demolding. After the peeling process, PDMS nanopillars became 10–60% longer in height than the mold size, and PDMS nanocones replica yields 150 % - 160 % larger in height compared to the mold size dimensions right before rupture. The experiment's observation gives the direction for this study to investigate the distortion of PDMS nanostructures in the demolding soft lithography process using molecular dynamics simulation. MD simulations found that PDMS nanocones at temperatures  $T=300$  K, 310 K and 320 K under uniaxial tensile stress show the characteristic of flexible plastic with noticeable yielding. The Ultimate Tensile Stress for PDMS nanocones ranges between 4.335 MPa - 6.478 MPa. MD simulations demonstrate that the PDMS nanopillar using 8 series and 12 series monomer under tensile stress also shows characteristics of flexible plastic with significant yielding. The PDMS nanopillar has a lower Young's Modulus, which are around 67–71 % of the bulk value. The Ultimate Tensile Stress for PDMS nanopillar is also about 46.3 % of the bulk value, and Poisson's Ratio is about 48.0 % compared to the bulk value.

# CHAPTER 1

## INTRODUCTION

### 1.1 Introduction

Nanotechnology has been the centre of research and development for many sectors, and it seems that in the era of industrial 4.0, nanotechnology existence has become more prominent. For the last 20-30 years, micro and nanodevices' demand has increased substantially as electric and electronic components become smaller. The needs of evermore-small devices have pushed micro/nanofabrication advancement for a better patterning, fabricating and replicating micro/nanostructures. Nanofabrication has been applied and revolutionized a wide range of area from the semiconductor industry to medicine and healthcare industries (Shi et al., 2010). Applications like nanoelectromechanical/microelectromechanical (NEMs/MEMs) devices, nano-optical devices and microfluidic have been a massive beneficiary from this advancement.

Nanoimprint lithography (NIL) was first introduced by Chou and co-workers (Chou, Krauss, and Renstrom 1995) in 1995 and has shown promising potential to produce low cost, high resolution, high throughput continuous nanostructures. NIL uses the simple concept of material displacement by mechanical contact. This method enables continuous pattern transfer from a mold to a target substrate.

Many research and studies have been conducted to optimize the fabrication process. However, most of the studies are concentrated on the experimental method. It is not deniable that experimental works give meaningful data for process

optimization and fabrication detailing. Still, there is one aspect of nanofabrication often neglected, which are fundamental science of the process. In order to fill in the gap, computational aided simulations are necessary to grasp the process's fundamental science. Methods that based on a continuum model such as Finite Element Analysis or Finite Volume Method is not suitable at the molecular level. Hence, a novel approach such as molecular dynamics simulation were employed to tackle this problem.

Molecular dynamics is a deterministic approach to calculate the dynamics trajectories of molecules, atom or ion. Molecular Dynamics has been used extensively in tribology, material properties and rheology. In molecular dynamics, the change of the molecular trajectories can be extracted and to be used to predict macroscopic behaviour. This method is a powerful tool to look the process changes at a molecular level.

## **1.2 Research background**

One of the biggest challenges in nanofabrication of devices is to optimize the processes to have constant output, and it is especially difficult for a high-resolution pattern. In nanofabrication, many factors can affect outcomes such as pressure, temperature and handling error. It is difficult to point out which element that cause which error. One of the method to find the flaw is by analyzing the failed output. This analysis was done by relating the distortion that is happened with the process that might have the error. Furthermore, for a technique like nanoimprint lithography (NIL) that employed demolding concept to produce high throughput, many other factors may distort the replications, such as temperature, pressure, aspect ratio and peeling-off technique (Guo 2007; Hamaya et al., 2018; Schiff 2008; Traub,

Longsine, and Truskett 2016). Although extensive studies have been carried out to study nanofabrication deformation, most of them are just observations from experimental results. Hence, a computational model is essential in simulating the process and provides useful information to understand and hopefully predict the process at a molecular level.

In this thesis, an attempt to model stress and strain of nanostructure using molecular dynamics (MD) is presented. In NIL, many factors could cause deformation on the replica. When all the factors are accumulated, the manufacturing process needs to understand the stress and strain relationship of a substrate in the demolding process. This project will study the demolding process using molecular dynamics simulation and its effect on the nanostructures deformation. The main interest of this project is the analysis of stress and strain relationship of the demolding process. Poly(dimethylsiloxane) or in short PDMS is chosen as an object of study because PDMS is widely used in NIL.

Molecular dynamics simulation can be divided into three stages. The first stage is to define the system. These include initial conditions (e.g. number of atoms, simulation's volume), boundary conditions and inter-atomic potential. At step two, new positions and velocities of atoms are calculated using the Newtonian equation. Macroscopic properties such as temperature and stress can be calculated using the updated position and velocity. At stage three, the time-averaged macroscopic properties are calculated.

### **1.3 Problem statement**

The main objective of the nanofabrication process is to obtain the desired profile within tolerance. However, most of the cases suggest the contrary. Many factors could cause the results to deviate from the desired profile, and due to the imaging limitation, the demolding process cannot be observed in real-time. In order to understand the influencing factors, a computational model is proposed. A computational model enables us to study the stress and strain relationship as the process proceeding. These include bond breaking, bond formation and atom rearrangements.

The actual nanofabrication process occurs at the molecular level and simulation methods that used the continuum model such as FEA that used Navier Stoke equation unable to model process at the molecular level (Rapaport 2004). From experimental observations, there many forms of deformation such as elongation, breakage, buckling (Hui et al., 2002). However, proper explanations are unable to be presented because of experimental and imaging limitations. Hence, one way of explaining the phenomena is by using computational modelling.

Thus, a novel approach is required to model the process at nano-scale. Several methods are available in nano-scale modelling. However, the most accurate and deterministic method is the Molecular Dynamics (MD) method. In this project, a MD model of PDMS under stress will be investigated. In MD method, the most crucial components is force field that model the forces between atoms within molecules. There are plenty of force field ranging from diatomic potential to many-body potential are available but there is no force field that can fit for all circumstances. The key of successful simulation in molecular dynamics is to find a force field that have suitable

parameter for the intended processes and material. For this project, two type of many-body force fields have been selected to model the stress and strain relationship of PDMS nanostructures under tensile. The force fields are Polymer Consistent Forcefield (PCFF) and Condensed-phase Optimized Molecular Potentials for Atomistic Simulation Studies (COMPASS) force.

#### **1.4 Research objective**

- a) To develop a computational model of the PDMS nanocones and nanopillar structures. These include the atoms' initial positioning, material structure, pre-determined external forces, bonding energy, and intermolecular forces.
- b) To utilize molecular dynamics (MD) simulation to study the stress and strain relationship of PDMS nanostructures under uniaxial tensile stress.
- c) To study the effects of temperature and chain length on the stress and strain relationship of nanocones.

#### **1.5 Scope of research**

This thesis is an attempt to find the explanation of distortion occur in soft lithography of PDMS nanostructures through computational method. The preliminary work for this project is to find the evidence of distortion occur in experimental works. The evidences found will then be used to form the hypothesis of this project. The experimental works will include sample preparation, electron beam lithography, soft lithography and surface characterization. All these steps will be discussed in details in Section 3.2.



After the experimental works and all required data are collected and analysed, the result will be used as guide for the computational simulation. In this part, the process include the building of the monomer, the building of nanostructure via packing process, the initial and boundary condition and the study of the nanostructure under tensile. The details of the simulation method will be discussed extensively in Section 3.3.

## **1.6 Thesis outline**

This thesis consists of five main chapters. Chapter 1 is the introduction of the thesis. This chapter will overview this thesis and a brief introduction to the research scope like the molecular dynamics (MD) methods and demolding process in nanoimprint lithography. A list of problem statements that will be investigated throughout this thesis will also be presented. The need to understand physical etching behaviour at the molecular level is thoroughly discussed.

Chapter 2 compiles all the works and research related to this project. At the beginning of the chapter, soft lithography and its usages are discussed. The concepts and demolding process in soft lithography was also introduced. These include the types of nanostructure distortions due to the demolding process. In this chapter, the force field used in this study are explained. These include the compilations of research that used these force fields.

In Chapter 3, all of the methodologies of this research will be presented. These include the details of building the basic structure of PDMS. The basic structure will be used as a building block to create a giant structure of PDMS. The building block of quartz is independently built as a mean to further our understanding of this topic. After

the substrates were built, the substrates will undergo several simulation tests. These simulations are conducted to fulfil the objectives of this thesis. Simulations are performed using Molecular Dynamics (MD) method. The details of the simulations will be covered in this chapter.

In Chapter 4, all the results obtained from all the methods in Chapter 3 are presented. The results from experimental works are presented at the beginning of the chapter. The observations from experimental works are used to give the framework for the MD simulations. For MD results, the first stage of MD which define the system are presented. These include energy minimization, temperature equilibrium and pressure equilibrium. After system initialization, results from the second and third stages are presented in the latter section. These include stress and strain relationship of PDMS nanopillar and nanocones, the effect of chain length and substrate temperature,  $T_s$ .

Chapter 5 gives the overall conclusion about this research. Recommendations are also presented for improving future and more extensive research on this subject.

In Appendix, Appendix A are the code for LAMMPS programming, Appendix B are the datasheet for Polymer Consistent Forcefield (PCFF) and Appendix D are the datasheet for Condensed-phase Optimized Molecular Potentials for Atomistic Simulation Studies (COMPASS) force.

## **CHAPTER 2**

### **LITERATURE REVIEW**

#### **2.1 Introduction**

This chapter comprises of two parts: The first part is soft lithography concept and the compilation of its research, development, and applications. The development in cell-nanotopography interaction and its application also presented in this part.

The later part is the compilation of works and research in molecular dynamics simulation related to soft lithography. This chapter also includes the work and research on the nanostructures distortion in experimental and simulation.

#### **2.2 Soft lithography and its applications**

There are many methods to make nanostructure, from precise fabrication like electron beam lithography, reactive ion etching and ion milling to random fabrication like anodizing, polishing and blasting techniques. Top-down fabrication techniques like electron beam lithography can achieve features down to 10 nm (Schleunitz et al., 2011). However, no matter how promising the prospects are, techniques like electron beam lithography, focus ion beam lithography and other ultraviolet lithography are very expensive and require expertise to produce the desired nanostructure (Guo 2007; Kooy et al., 2014; Liu et al., 2011). Furthermore, these techniques are inefficient, thus not suitable for mass production.

In order to drive innovations and research in nanofabrication technology, a low cost, high resolution, high throughput nanolithography technique is necessary. Rapid development in the semiconductor industry has dramatically advanced the innovations of micro/nanofabrication techniques. Methods like nanoimprint lithography (NIL) and

electrospinning enable researchers to build and fabricate nanostructure at a larger substrate at a lower cost. A study conducted by Sclunitz and co-workers (Schleunitz et al., 2011) has succeeded to continuously imprinted 40 meters of 200 nm depth, and width nanograting on cellulose acetate thermal resist using nanoimprint lithography. Nanoimprint lithography (NIL) was first introduced by Chou and co-workers (Chou et al., 1995) in 1995 and has shown promising potential to produce low cost, high resolution, high throughput continuous nanostructures. NIL uses the simple concept of material displacement by mechanical contact, as shown in Figure 2.1

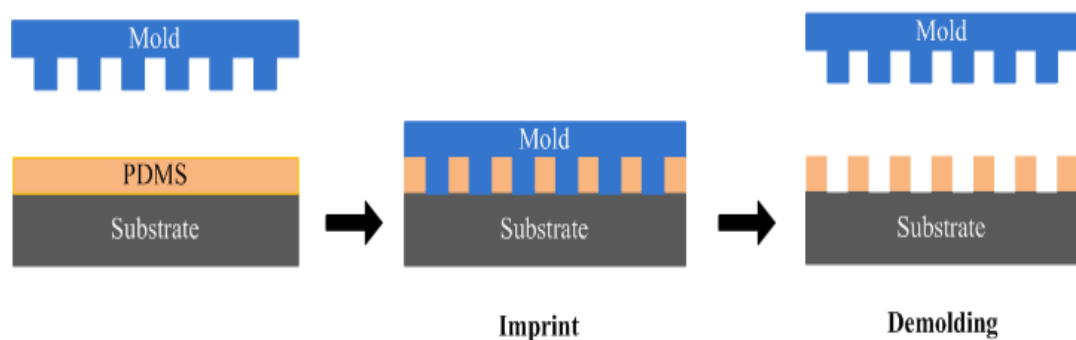


Figure 2.1 Soft lithography uses in NIL a) Imprint process and b) Demolding process

In NIL, the fabricated mold is printed onto a resist using specialized printing equipment (Torres 2003). When using this method, the mold is fabricated once using precise fabrication techniques like electron beam lithography (Chen et al., 2006) or focused ion beam (Taniguchi et al., 2006) and using the mold as a master mold. The nanostructure can be replicate repetitively by imprint it to the suitable material. This method enables continuous pattern transfer from a mold to a target substrate. While the concept is simple, many factors may distort the replications, such as temperature, pressure, aspect ratio and peeling-off technique (Guo 2007; Hamaya et al., 2018; Schiff 2008; Traub et al., 2016). Thus, when all distortion factors are accumulated, it is vital

in the manufacturing process to understand the stress and strain relationship of a substrate in the demolding process.

Figure 2.2 shows the comparison between two types of NIL based on resist curing; thermal nanoimprint lithography (hot embossing) and ultraviolet (UV) nanoimprint lithography. For thermal nanoimprint lithography, the imprint mold is heated slightly higher than the heat glass transition temperature,  $T_g$  of the resists. The heated mold will soften the resist, and the viscous resist will fill the cavities and form the mold's reverse pattern. After that, the mold is cold to a temperature below  $T_g$  of the resist and then separated. In UV nanoimprint lithography, the resist is cured using UV light exposure at room temperature, and separation occurs at room temperature without elevated temperature.

Contrary to thermal NIL that manipulates phase change corresponded to the temperature, UV-NIL causes resist hardening by increasing the cross-linking in the UV-sensitive polymer (Colburn et al., 1999). UV-NIL requires smaller imprint pressure compare to thermal NIL because of the uses of less viscous photoresist (Lee et al., 2008; Vogler et al., 2007). Apart from thermal NIL and UV-NIL, NIL variants used both thermal and UV curing like the simultaneous thermal and UV (STU<sup>®</sup>) developed by Obducat Technologies (Anon n.d.). These techniques enable the NIL cycle been conducted at constant temperature by using both thermal curing and UV curing simultaneously (Chen 2015).

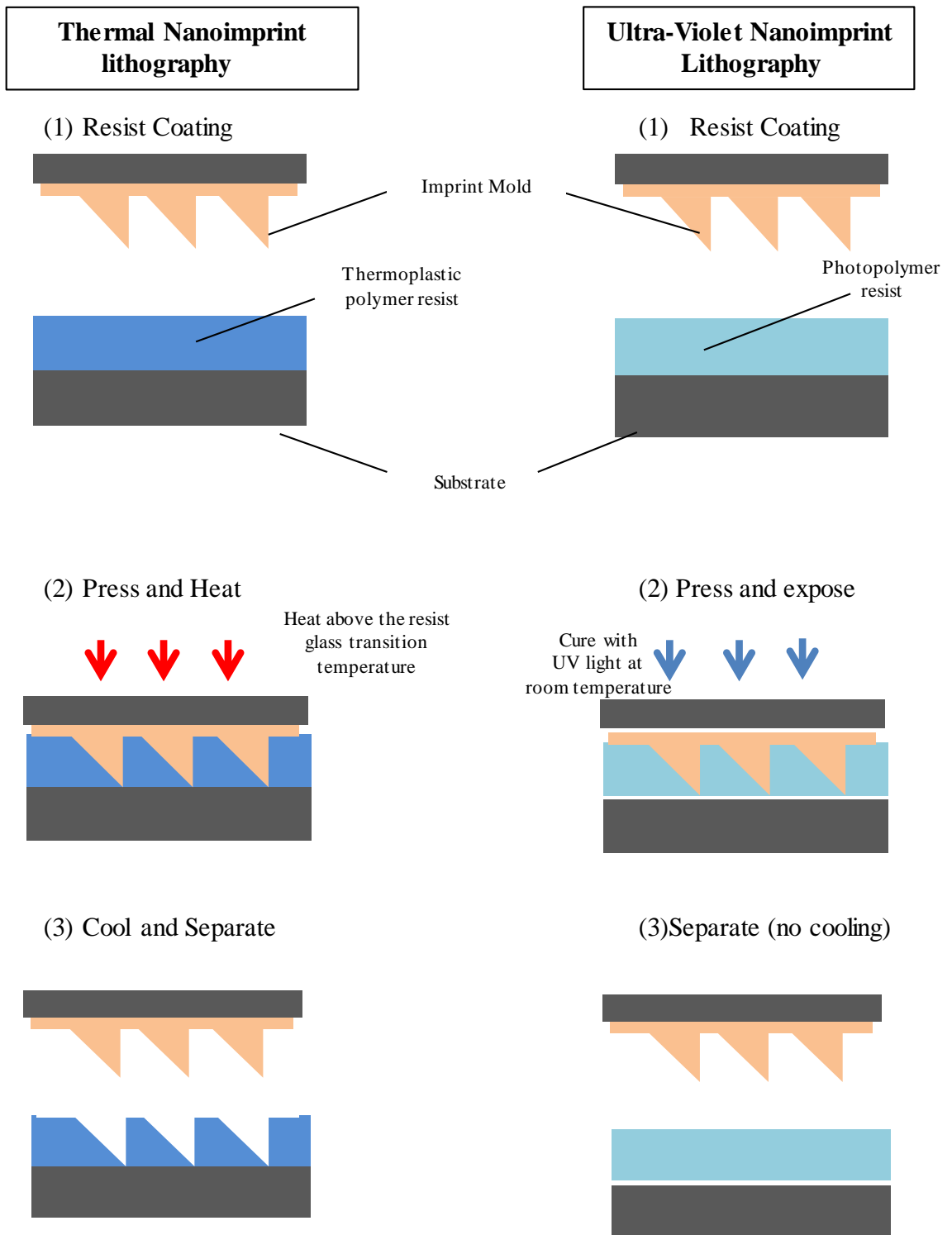


Figure 2.2 Comparison of Thermal Nanoimprint Lithography (Thermal NIL) and Ultra-Violet Nanoimprint Lithography (UV NIL)

There are also three variants of NIL based on imprint contact. Namely are plate-to-plate (P2P), roll-to-plate (R2P) and roll-to-roll (R2R). Figure 2.3 gives the illustrations differences between the three NIL. In term of prospect for mass production, R2R NIL offers a promising future for industry-scale applications. R2R NIL concepts are based on roll-to-roll manufacturing processes. Thus this technique can produce continuous and high throughput products (Ahn and Guo 2008; Lan et al., 2008). R2R NIL has more significant advantages than conventional P2P NIL in terms of size of the equipment, output and imprint force (Song et al., 2010). Table 2-1 shows a summary of various studies and research using different NIL to fabricate nanostructures. Table 2-1 summarized the various studies that used different technique of nanoimprint lithography. From Table 2-1 the final product of nanostructure imprinted a ranging between sub-10nm to more than 100nm. Study by Liang and co-workers obtained a ribbon of hexagonal graphene nanomesh with dimension of sub-10nm (Liang et al., 2010). This show the huge potential of nanoimprint lithography in producing micro/nanostructure at industrial scale.

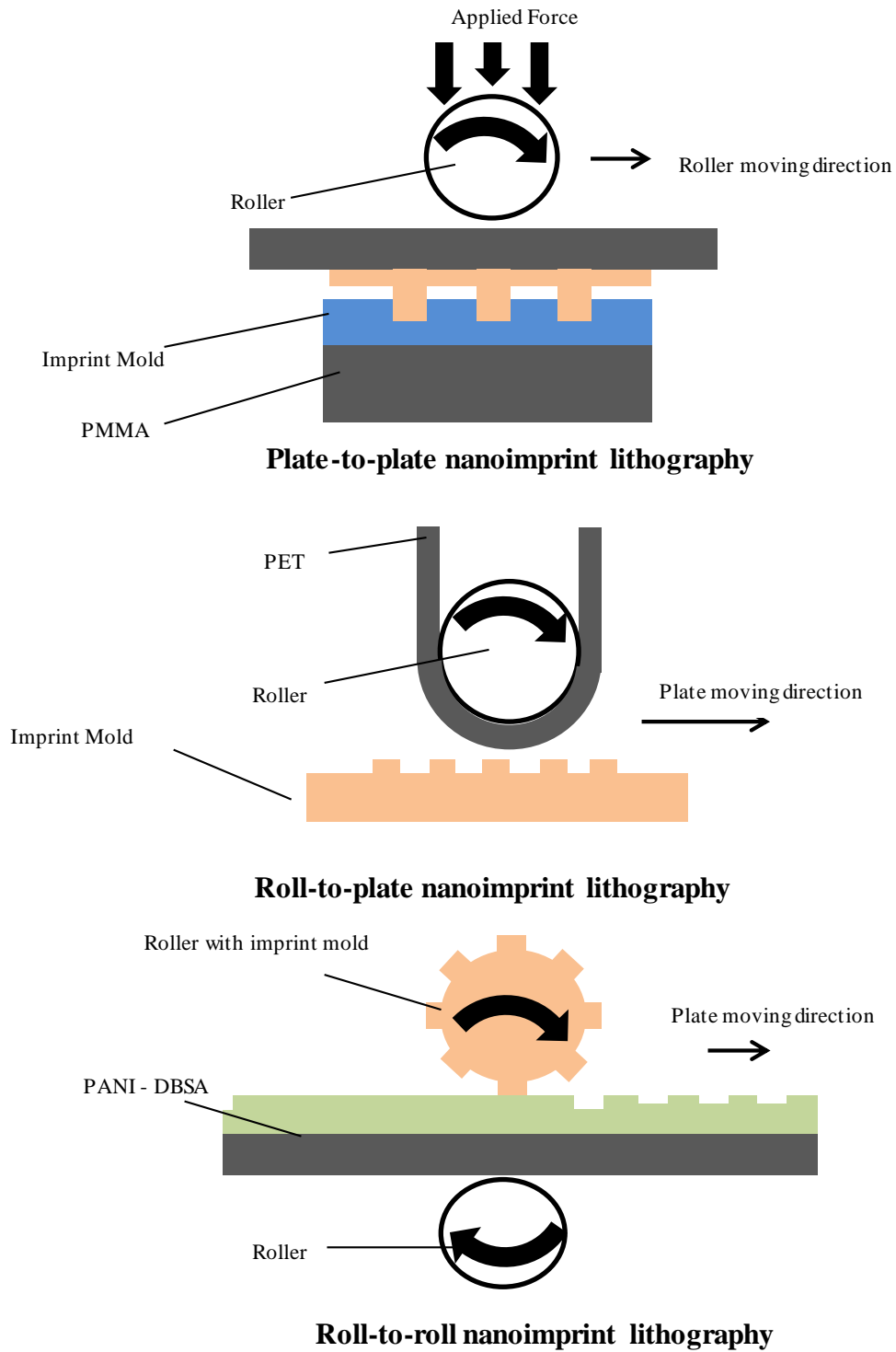


Figure 2.3 Nanoimprint variation based on imprint techniques



Table 2-1 Summary of various studies that using different technique of nanoimprint lithography

<b>Researcher</b>	<b>NIL</b>	<b>Resolution</b>	<b>Mold</b>	<b>Resist</b>	<b>Final Product</b>
Liang and co-workers (Liang et al., 2010)	P2P	Sub-10 nm of ribbon width	SiO <sub>2</sub> (quartz) template	Polystyrene	Sub-10nm width ribbon of hexaganol graphene nanomesh (GNMS)
Shinohara and co-workers (Shinohara et al., 2008)	P2P	120 nm diameter of nanodot	SiO <sub>2</sub> (quartz) template	TR-21 from Tokyo Gosei Co. Ltd.	120 nm diameter of CoPt nanodots
Ye and co-workers (Ye et al., 2010)	P2P	sub-100 nm of periodic nanoline and array of nanodot	Hydrogensilsesquioxane (HSQ)	Polyset® epoxy siloxane nanoimprint resist from Polyset Company Inc., Mechanicville, New York, USA	50nm lines and dot with high aspect ratio are successfully replicated using PDMS soft mold.
Tan and co-workers (Tan, Gilbertson, and Chou 1998)	R2P	sub-100 nm of nanograting	Thin Ni film	PMMA	Sub-100 nm of PMMA nanogratings
Ahn and co-workers (Ahn and Guo 2009)	R2P	300 nm line width of nanograting	Ethylene Tetrafluoroethylene (ETFE)	Epoxy silicone	300 nm line width and 600 nm of epoxy silicone nanogratings
Schleunitz and co-workers (Schleunitz et al., 2011)	R2R	200 nm line width of nanograting	OrmoStamp coated with anti-sticking layer (ASL)	Cellulose Acetate (CA) film	200 nm depth and width of CA. (A continuous 40 m of CA printed)

### **2.2.1 Development in cell-nanotopography interaction and its application**

This thesis is part of a larger project of collaborative work in nanotechnology application in healthcare. Rapid development in nanofabrication has opened up many possibilities of applications for cell-nanotopography interaction. Robert Langer in his work stated that nanotechnology may revolutionize and change the pharmaceutical industries (Shi et al., 2010).

Cells in general are in micro scale and cell contact response (contact guidance) with native topographic structure was first studied in 1911 by Harrison (Harrison 1911). Contact guidance has been studied and defined since when it was first observed in 1911 (Weiss and Garber 1952). Interestingly, cell gives different response when it interacts with surface that has smaller structures than itself for example structure at nano scale. Many of the responses are beneficial and it can be used as a tool to direct cell action (Haga et al., 2005; Sutherland, Denyer, and Britland 2005). Nanostructure that in contact with cell can act as mechanosensory and send signals for cell adhesion, differentiation and proliferation (Haga et al., 2005; Sutherland et al., 2005). The knowledge of cell adhesion with nanotopographic structure is the most important part to understanding cell-nanotopography interactions (Dalby, Gadegaard, and Oreffo 2014). Other responses are meaningless if cell does not adhere onto a surface. There are many studies that have been conducted with many kinds of nanotopographic structure. From cell interaction with precise, highly symmetric nanostructure (Gallagher et al., 2002; Lee, Mazare, and Schmuki 2014), randomized nanostructure (Anselme et al., 2010), and disordered nanostructure (Anselme et al., 2010).

Since the first hematopoietic stem cell (HSC) transplantation 50 years ago, many studies have been conducted to study stem cell including its interaction with nanotopography (Parekkadan and Milwid 2010). Stem is particularly interested to many researchers because of its ability to differentiate into multiple mature cells (Jung, Bauer, and Nolta 2012). The main goal in stem cell research is to control stem cell differentiation into specific cell lineage. The differentiation of mesenchymal stem cells (MSCs) can be regulated using the interactions of cell to nanotopography (Filova et al., 2015; Oh et al., 2009; Park et al., 2007). Human embryonic stem cells (hESCs) also show the same interaction when placed on nanotopography. Nanotopological mechanosensory of hESCs significantly affect cell spreading, adhesion and self-replication (Gerecht et al., 2007).

The interaction of hSEC with nanotopography opens a huge application in tissue engineering and medical application because the unique characteristic of hSEC (pluripotency) that can be differentiated to specialized human cell (Jaenisch and Young 2008; Keller 2005). Extensive studies have been conducted to study the cell interactions with TiO<sub>2</sub> nanotube. Cells respond includes adhesion, proliferation and apoptosis depending to the size of nanotube. Study by Park and co-workers (Park et al., 2007) shows that cell adhesion and proliferation are maximum at nanotube with the diameter of 15nm and cell apoptosis at diameter 100nm.

Many studies agree that cell fate are dictated within the threshold value of nanotube size 30-50nm (Oh et al., 2009; Park et al., 2007). Surface with nanotube diameter that are larger than 50nm will cause cells to impair and limiting cell spreading and adhesion, regardless of any surface (Arnold et al., 2004; Popat et al., 2007). While

large nanotube (diameter >50nm) impairing cell to spread and adhesion, it evoke stem cell to elongate (Tsimbouri et al., 2014). The elongated mesenchymal stem cell (MSCs) will change its cytoskeletal structure due to high tension state hence produce osteoblast-like-cell (Lee et al., 2014). This discovery opens window of new development in nanotechnology specifically in orthopaedic treatment.

In term of the choosing on nanotopography, there are three options of nanostructures. First approach is to study the cell interaction with symmetric, highly precise nanostructure (Choi et al., 2007; Dalby et al., 2004), second approach is to study the cell interaction with randomize nanoscale roughness (Sjöström et al., 2009) and third approach is that take the middle route between precise and random is disorder nanotopography (Dalby et al., 2007). Cell interaction with precise nanotopography generally produce lower cell adhesion compare to random nanoscale roughness (Dalby et al., 2004; Leven, Viridi, and Sumner 2004). Although it is interesting to note that study by Laura and co-workers (McMurray et al., 2011) show that a precise symmetric al nanopits can retain hMSCs phenotype and multipotency for a long term of period (eight weeks). On the other hand, study by M.J. Dalby and co-workers (Dalby et al., 2007) show that the interaction between MSCs and disorder nanotopography resulted rapid osteogenesis which are comparable with the results of using corticosteroid ( i.e Dexamethasone) as bone formation inducing agent.

Table 2-2 show the summary of cell response to precise and symmetric nanostructures, Table 2-3 show the response of cell to randomize nanostructure and Table 2-4 show the summary of cell response to disorder/irregular nanostructure. The response can be categorized by the main response which are adhesion, proliferation and elongation of the cell. Column last of each table summarized other response such as differentiation.

Table 2-2 Summary of cell response to precise, highly symmetric nanostructures

Structure Type	Feature size	Cell Type	Substrate Material	Adhesion	Proliferation	Elongation, alignment	Other
Nanogrooves (Kim et al., 2013)	1. Width = 550nm 2. Spacing Gap = 550nm, 1650nm and 2750nm	hMSCs	PUA co-culture with HUVECS	hMSCs and HUVECS fully adhered the substrata	No significant different with flat substrate	hMSCs and HUVECS oriented along the nanopattern. CEF 2-3 times higher than flat surface.	Osteogenesis highest at space gap 1650nm
Nanogratings (Yim et al., 2010)	1. Width = 350nm and 500nm 2. Pitch = 700nm and 1µm 3. Depth = 350nm	hMSCs	PDMS	hMSCs cultured on nanograting show decreased in integrin subunits	-	hMSCs aligned and elongated on nanograting while on flat surface cell spread randomly	hMSCs FA and F-actin affected by substrate stiffness and topography
Nanopillar and nanowell (Muhammad et al., 2015)	1. d = 356nm pillar 2. d = 1.38µm wells 3. d = 1.80µm pillars	HCECs	TCPS coated with FNC or LC	-	All substrates yield higher proliferation rate than plain substrate. HCECs on 1µm FNC-coated pillars produce significantly higher proliferation rate with 2.9 folds.	In p-media, HCECs elongated and in s-media HCECs fully confluent and maintain the native shape	Nanotopographic memory help HCECs sustain functional marker
Nanopost (Ahn et al., 2014)	1. d = 700nm 2. Spacing Gap = 1.2, 2.4, 3.6 and 5.6µm	hMSCs	PUA	hMSCs surface contact area decrease at denser nanopost	-	-	hMSCs at denser nanopost favoured osteogenesis and hMSCs at less denser nanopost favoured adipogenesis

Table 2-3 Summary of cell response to randomize nanostructures

Structure Type	Feature size [a]	Cell Type [b]	Substrate Material [c]	Adhesion	Proliferation [d]	Elongation, alignment	Other [e]
Nanorough-ness (Chen et al., 2012)	$R_q$ between 1nm to 150nm	hESCs	Glass coated with vitronectin	Decrease with $R_q$ increase	Doubling time increase with $R_q$ increase	hESCs on high $R_q$ are more compact and shorter cytoplasmic extension.	hESCs differentiation increase on rough surface
Microfiber with ellipse shaped nanopores surface (Zhou et al., 2015)	1. $d_f = cs$ . 1.6 $\mu$ m 2. $AR_{\text{ellipse}} = 2.7-3.9$ (54.8 – 110.0nm)	vSMCs	PLLA microfiber with nanopores surface	After 8 hours cultured, the number of attached vMSCs increased.	After 7 days, cultured, PLLA fiber shown to support cell proliferation	After 8 hours cultured, cell elongated	Nanopores on the microfiber surface increase cell bio-mimics. Improve adhesion, proliferation and the synthesis of vascular protein matrix.
1. Cylindrical microfiber with smooth (CS) and porous (CR) surface 2. Ribbon microfiber with smooth (RS) and porous (RR) surface (Zamani et al., 2013)	1. $R_{q(CR1)} = 418\text{nm}$ 2. $R_{q(CR2)} = 182\text{nm}$ 3. $R_{q(CS)} = 170\text{nm}$ 4. $R_{q(RR1)} = 160\text{nm}$ 5. $R_{q(RR2)} = 363\text{nm}$ 6. $R_{q(RS)} = 366\text{nm}$	NCs	PLGA	Rough fibre increase adhesion	Proliferation correlated with roughness parameter obtained. A linear model of cell proliferation obtained based on five roughness parameters of $S_p, S_{sk}, S_q, S_m$ and $S_a$	-	Scaffold make from PLGA does not increase the toxicity level in the culture medium.
Nanorough-ness (Kato et al., 2014)	$R_c = 22\text{nm}$	hMSCs	Ti	-	-	-	20miRs specific marker upregulated by two fold by

									hMSCs grown on Ti with nanoroughness. This shown that chemically produced nanoroughness on Ti surface induced osteogenesis.
Precise spatially nanorough-ness (Chen, Sun, and Fu 2013)	R <sub>q</sub> between 1nm to 150nm	NIH/3T3	Glass	NIH/3T3 adhered at glass with R <sub>q</sub> = 70nm but not at smooth surface glass.	Proliferation increase significantly at rough surface.	NIH/3T3 at smooth surface has more cytoplasmic extension than high R <sub>q</sub> glass.			Nanotopgraphy induce cell mechanosensitivity thus decrease NIH/3T3 CSK contractility.



Table 2-4 Summary of cell response to disorder/irregular nanostructure

Structure Type	Feature size	Cell Type	Substrate Material	Adhesion	Elongation, alignment	Other
Nanopit (Pemberton et al., 2015)	1. d= 120nm 2. depth= 100nm	MSCs	Polycarbonate	-	-	Osteoblastogenesis occur in two different mechanism which are induced by nanotopography and piezo-stimulated mechanotransduction
RGD nano-pattern (Huang et al., 2009)	1. Spacing = 55-101 nm 2. h <sub>RGD</sub> = 10nm	MC3T3-E1	Glass	Disordered nanopattern gave better cell adhesion than ordered nanopattern. This is because disorder nanopattern has wider range of ligand density.	-	Intergrin clustering and adhesion by RGD ligand happen when ligand spacing is larger than 70nm
Nanotube (Oh et al., 2009)	1. d = 30, 50, 70, 100nm	hMSCs	Ti	1. Nanotube with d=30nm promote adhesion without differentiation 2. Number of adhered cell is inversely proportional to the nanotubes size.	1. hMSCs at 100nm TiO <sub>2</sub> nanotubes elongated 10 times larger than at 30nm TiO <sub>2</sub> . 2. Larger diameter nanotube promote osteoblastic differentiation	Cell adhesion and cell elongation are inversely related.

In order to utilise the interaction between cell and nanotopography, the understanding of cell adhesion maybe is the most important part. Cell adhere to a surface through a cellular adhesion receptor called integrin. Cell respond differently to variation of surface chemistry (Geiger, Spatz, and Bershadsky 2009), substrate stiffness (Engler et al., 2006), mechanical force (Rumpler et al., 2008) and surface topography (Dalby et al., 2002). In describing cell adhesion, Dalby and co-workers (Dalby et al., 2014) give analogy that cell is like a tent, and the pegs is the integrin cluster that hold the tent to the ground. However, cell can chose to where it wants to harbour the integrin cluster by changing its cytoskeleton. When the surface has the nanostructure that are comparable scale to the cell integrin, a signal can be given to the cell through the integrin. Focal adhesion are the organelles that are mediate signal (Bershadsky, Balaban, and Geiger 2003) ,regulate cytoskeletal change (Mitra, Hanson, and Schlaepfer 2005) and adhesion (Geiger et al., 2001) when cell in contact with ECM. Kanchanawong and co-workers (Kanchanawong et al., 2010) show that focal adhesion is ~40nm multi protein-specific strata region in between integrin and actin and consist of well-organized molecular architecture. FAK (Focal adhesion kinase)was found in 1992 and describe as highly tyrosine-phosphorylated protein (Guan and Shalloway 1992). FAK and Paxilin represent the membrane proximal integrin signalling that mediate adhesion, controlling the cytoskeleton and regulate cell movement (Kanchanawong et al., 2010).

The cell response to the nanostructure can be utilized in many ways. One of such application is the development of antimicrobial surfaces. Such surfaces can be found naturally such as in dragonfly wing (Ivanova et al., 2013) and gecko skin (Watson et al., 2015) and researcher around the world try to replicate these surfaces in lab setting. For instance, a research by Ivanova and co-workers found that dragonfly wing which

has surface of nanocones with the dimension of 50-70 nm in base diameter, with height of 240nm show clear sign of antibacterial property (Ivanova et al., 2013). Another study by Kelleher et al., observed that nanopillar found on cicada wing has an effective antimicrobial property against gram negative bacteria, *P-aeruginosa*.

### **2.2.2 Polydimethylsiloxane in Soft Lithography**

Polydimethylsiloxane or in short PDMS is common and commercially available inorganic elastomer used extensively in micro/nanostructure fabrication or lithography. PDMS's monomer has a siloxane backbone with methyl group attached to the silicon.

PDMS has a mechanical and chemical properties that make it suitable for micro/nano fabrication especially soft lithography. In room temperature, PDMS is in fluid and solidify when heated. PDMS also has unique properties where it can make conformal coating with most surface and can easily peel off from that surface. Furthermore, PDMS can act as membrane to allow gasses to pass through and it does not swell with humidity (Whitesides 1996). In term of chemical properties, PDMS is chemically inert, has low interfacial energy and has high transparent depth up to 300 nm (Hawkins and Schmidt 2010). This properties make PDMS ideal to used as replica material for high aspect ratio nanostructure.